

Bayesian Iterative Closest Point for Shape Analysis of Brain Structures

Mauricio Castaño-Aguirre^{1,2}^a, Hernan F. Garcia^{3,1}^b, Álvaro A. Orozco²^c,
Gloria Liliana Porras-Hurtado¹^d and David A. Cárdenas-Peña²^e

¹Salud Comfamiliar, Comfamiliar Risaralda, Pereira, Colombia

²Automatics Research Group, Universidad Tecnológica de Pereira, Pereira, Colombia

³SISTEMIC Research Group, Universidad de Antioquia, Medellín, Colombia

Keywords: Bayesian Optimization, Gaussian Processes, Iterative closest-Point, Point Cloud Alignment, Shape Analysis.

Abstract: Machine learning in medical image analysis has proved to be a strategy that solves many problems emerging from the variability in the physician's outlines and the amount of time each physician spends analyzing each image. One of the most critical medical image analysis approaches is Medical Image Registration which has been a topic of active research for the last few years. In this paper, we proposed a Bayesian Optimization framework for Point Cloud Registration for shape analysis of brain structures. Here, we rely on a modified version of the Iterative Closest Point (ICP) algorithm. This approach built a black box function that receives input parameters for performing an Point Cloud transformation. Then, we used a similarity metric that shows the performance of the transformation. With this similarity metric, we built a function to define a Bayesian strategy that allows us to find the global optimum of the similarity metric-based function. To this end, we used Bayesian Optimization, which performs global optimization of unknown functions making observations and performing probabilistic calculations. This model considers all the previous observations, which prevents the strategy from falling into an optimal local, as often happens in strategies based on classical optimization approaches such as Gradient Descent. Finally, we evaluate the model by performing a point cloud registration process corresponding to brain structures at different time instances. The experimental results show a faster convergence towards the global optimum and building. Besides, the proposed model evidenced robust optimization results for registration strategies in point clouds.

1 INTRODUCTION

Image registration is the preferred technique in medical image applications and has been a topic of active research over decades. Medical image registration techniques serve as the fundamental basis for procedures such as image-guided radiation therapy, image-guided radiation surgery, and image-guided minimally invasive treatments (Wang et al., 2014; Jaffray et al., 2007; Sadozye and Reed, 2012). Intuitively, the registration process finds an optimal transformation that aligns an image in the input data and is a crucial step for image analysis; in which valuable information is conveyed in more than one image (i.e., images acquired at different times). Therefore, accurate inte-

gration of relevant information from two or more images is very important (Oliveira and Tavares, 2014). In the context of registration processes, fixed image remains unchanged, and the moving image is transformed using the fixed Image as a reference (Oliveira and Tavares, 2014).

Most of the works currently carried out in medical image registration are based on deep learning strategies. However, these approaches are time-consuming and lack interpretability. Since the discovery of deep learning applications in the context of segmentation and classification tasks, new applications have emerged; for example, a Deep Learning Image Registration framework for unsupervised affine and deformable image registration is proposed (Vos et al., 2019). In this framework, a convolutional neural network (ConvNet) is trained for image registration by exploiting image similarity analogous to conventional intensity-based image registration. After the ConvNet has been trained, it can register pairs of unseen images

^a <https://orcid.org/0000-0002-2811-7847>

^b <https://orcid.org/0000-0002-2814-8838>

^c <https://orcid.org/0000-0002-1167-1446>

^d <https://orcid.org/0000-0003-1193-7184>

^e <https://orcid.org/0000-0002-0522-8683>

in one shot. Similarly, other strategies (Mansilla et al., 2020) build a function to model images as a deformation field that aligns multivariate views. This model is a fast learning-based framework for deformable, pairwise medical image registration. In addition, the strategy rapidly computes a deformation field by directly evaluating the function (Mansilla et al., 2020).

Although most deformable image registration strategies use deep learning-based image registration methods (Balakrishnan et al., 2019; Krebs et al., 2019; Lau et al., 2020; Mansilla et al., 2020; Vos et al., 2019; Zhao et al., 2019) achieving state-of-the-art performances. However, The proper interpretability of the deformation process is still an open gap in the image registration field. Similarly, this model requires a time-consuming training phase and a large amount of data to perform well in the validation. Consequently, the model leads to problems in which there is insufficient sample quantity in the input data. Regardless, local pixel-level loss functions do not consider the global context and might produce similar values for anatomically plausible, and non-plausible segmentation. Also, these strategies rely on 2D approaches in which each slice of the medical image is processed, restraining the correspondence information between shapes.

Point cloud registration methods such as Iterative Closest Points (ICP) have been successfully applied in numerous real-world tasks (García et al., 2016; Besl and McKay, 1992; Chen and Medioni, 1991; Liu et al., 2016; Oomori et al., 2016; Umeyama, 1991; Zhang, 2005; Zhang et al., 2022; Li et al., 2022; Bouaziz et al., 2013). This strategy is known for its susceptibility to local minima problems and requires adequate model initialization and manual hyperparameter tuning. Therefore, a proper model optimization is required to perform accurately.

In (García et al., 2016) the use of optimization models to fit 3D brain structures based on Bayesian optimization has been explored. However, due to emerging problems related to the classical Bayesian optimization approach such as misspecified models and covariate shift we can identify a need to define optimization strategies that allow us to deal with these problems. Bayesian Optimization (BO) reaches global optima in many challenging optimization benchmark functions (Jones, 2001). BO states that the objective function is sampled from a Gaussian Process, maintaining the posterior distribution for this function as observations. Recently, new strategies have improved Bayesian Optimization by reducing the iterations required for the convergence by adding stopping criteria for the searching process (Dai et al., 2019; Stanton et al., 2022; Fong and Holmes, 2021),

which makes this type of strategy even more efficient for global optimization processes.

This paper proposes a point cloud registration approach to building a black box function based on an point cloud transformation optimization within a Bayesian framework. Here, we use Bayesian optimization to find the optimal parameters that align the point clouds accurately. Our key contribution is based on the Bayesian optimization strategy that computes the model parameters for controlling the alignment of the point cloud registration process in a probabilistic way. The rest of the paper proceeds as follows. Section 2 provides a detailed discussion of materials and methods. Section 3 presents the experimental results and some discussions about the proposed method. The paper concludes in Section 4, with some insights about the proposed framework.

2 MATERIALS AND METHODS

2.1 Datasets

For the input data, we use two databases. The first is the Tosca dataset (Bronstein et al., 2006), a dataset with Hi-resolution three-dimensional nonrigid shapes. The database contains 80 objects, including 11 cats, 9 dogs, 3 wolves, 8 horses, 6 centaurs, 4 gorillas, 12 female figures, and two different male figures, containing between 7 and 20 poses (Bronstein et al., 2007). Furthermore, the second one comes from Magnetic Resonance Images (MRI) from patients with perinatal asphyxia acquired during early childhood in a medical center in Colombia called Brain Asphyxia Dataset. The MRI images are then converted into 3D point cloud data using the infant Free Surfer framework (Fischl, 2012). Then, we obtain segmentations of 20 different neuroanatomical regions relevant in the context of perinatal asphyxia (Satheesan et al., 2020), (Miller et al., 2005). After this process, the anatomy of a subject is represented by a collection of m ($m = 20$ brain structures) point clouds $S = \{P_0; P_1; \dots; P_m\}$, where each point cloud represents a brain structure. A point cloud is defined as a set of n points $P = [P_0; P_1; \dots; P_n]$, where each point is a vector of coordinates $P_i = (x, y, z)$ (Gutiérrez-Becker and Wachinger, 2018).

We test our approach in 20 different point clouds for the Tosca data sets. In this data set, we applied a rigid random transformation to evaluate if the model can find rigid transformations on point clouds with significant variability. For the perinatal asphyxia dataset, we test our model with MRI acquired at different times related to the same patient (i.e., to evalu-

ate the clinical outcome). Each patient has 20 different neuroanatomical structures at different ages (e.g., at birth and one year). Among these structures, we have left and right white matter, caudate nucleus, putamen, and thalamus.

2.2 Transformations for 3D Point Clouds

As for the implementation of the registration algorithm, we rely on the ICP algorithm used in (Rusinkiewicz, 2001). Then, we build a function to model variables for translational and rotational parameters.

We must define the constraints of the transformation function to guarantee an optimal grid search. For the rotational parameters, we define constraints from -2π to 2π , and the translations parameters are given by,

$$\alpha = \{\alpha \in \mathbb{R} \mid -2\pi \leq \alpha \leq 2\pi\} \quad (1)$$

$$\beta = \{\beta \in \mathbb{R} \mid -2\pi \leq \beta \leq 2\pi\} \quad (2)$$

$$\gamma = \{\gamma \in \mathbb{R} \mid -2\pi \leq \gamma \leq 2\pi\} \quad (3)$$

$$t_{x,y,z} = \{t \in \mathbb{R}\}. \quad (4)$$

Then, the transformation matrix with rotational parameters α, β, γ and the translations for each axis $t_{x,y,z}$ are,

$$\mathbf{T} = \begin{pmatrix} \cos \alpha \cos \beta & \cos \alpha \sin \beta \sin \gamma - \sin \alpha \cos \gamma & \cos \alpha \sin \beta \cos \gamma + \sin \alpha \sin \gamma & t_x \\ \sin \alpha \cos \beta & \sin \alpha \sin \beta \sin \gamma + \cos \alpha \cos \gamma & \sin \alpha \sin \beta \cos \gamma - \cos \alpha \sin \gamma & t_y \\ -\sin \beta & \cos \beta \sin \gamma & \cos \beta \cos \gamma & t_z \\ 0 & 0 & 0 & 1 \end{pmatrix} \quad (5)$$

2.3 Performance Metric

To set the optimization process, we need to use a performance metric that measures the similarity or the differences between the objects to be aligned. We use Root Mean Square Error and Normalized Mutual Information (MI). MI measures objects' information, as shown in equation 6,

$$I(P_A, P_B) = D_{KL}(P_{(A,B)} \| P_A \otimes P_B), \quad (6)$$

where D_{KL} is the Kullback–Leibler divergence (Williams and Maybeck, 2006). If this information is zero, it means that knowledge on B does not give any information about A (i.e., two partitions have nothing to do with each other). The larger the two partitions are, the larger $I(P_A, P_B)$. However, this is still not an ideal metric for evaluating. Thus, we choose to normalize it as in $H(P_A) + H(P_B)$ (see (Zhang, 2015) for further details). The Normalized Mutual Information can be written as

$$NMI(P_A, P_B) = \frac{2I(P_A, P_B)}{H(P_A) + H(P_B)} \quad (7)$$

In this context A and B represents the fixed and the moving point cloud respectively.

2.4 Conformal Bayesian Optimization with Gaussian Process Priors

Our goal is to minimize the distance between the fixed and moving point cloud which is referred to as the cost function $f(\mathbf{x})$ on some bounded set \mathcal{X} that controls the model parameters. To this end, Bayesian optimization builds a probabilistic framework for $f(\mathbf{x})$ with the aim to exploit this model to make predictions about the transformation parameters $\mathcal{X} = \{\alpha, \beta, \gamma, t_{x,y,z}\}$ (Snoek et al., 2012).

The main components of the Bayesian optimization framework are the prior function to optimize and the acquisition function that will allow us to determine the next point to evaluate the cost function (Rasmussen and Williams, 2005). We use a Gaussian process prior due to its flexibility and tractability. A Gaussian Process (GP) is an infinite collection of scalar random variables indexed by an input space such that for any finite set of inputs $\mathbf{X} = \{\mathbf{x}_1, \mathbf{x}_2, \dots, \mathbf{x}_n\}$, the random variables $\mathbf{f} \triangleq [f(\mathbf{x}_1), f(\mathbf{x}_2), \dots, f(\mathbf{x}_n)]$ are distributed according to a multivariate Gaussian distribution $\mathbf{f}(\mathbf{X}) = \mathcal{GP}(m(\mathbf{x}), k(\mathbf{x}, \mathbf{x}'))$. A GP is completely specified by a mean function $m(\mathbf{x}) = \mathbb{E}[f(\mathbf{x})]$ (usually defined as the zero function) and a positive definite covariance function given by $k(\mathbf{x}, \mathbf{x}') = \mathbb{E}[(f(\mathbf{x}) - m(\mathbf{x}))(f(\mathbf{x}') - m(\mathbf{x}'))^T]$ (see (Snoek et al., 2012) for further details). Let us assume that $f(\mathbf{x})$ is drawn from a Gaussian process prior and that our observations are set as $\{\mathbf{x}_n, y_n\}_{n=1}^N$, where $y_n \sim \mathcal{N}(f(\mathbf{x}_n), \mathbf{v})$ and \mathbf{v} is the noise variance. The acquisition function is denoted by $a: \mathcal{X} \rightarrow \mathbb{R}^+$ and establishes the point in \mathcal{X} that is evaluated in the optimization process as $x_{\text{next}} = \arg \max_{\mathbf{x}} a(\mathbf{x})$. Since the acquisition function depends on the GP hyperparameters, θ , and the predictive mean function $\mu(\mathbf{x}; \{\mathbf{x}_n, y_n\}, \theta)$ (as well as the predictive variance function), the best current value is then $x_{\text{best}} = \arg \min_{\mathbf{x}_n} f(\mathbf{x}_n)$.

Since the discovery of the problems encountered in the classical Bayesian optimization models like model misspecification and covariate shift. It is necessary to find strategies that try to solve this problem as it does Conformal Bayesian Optimization (Fong and Holmes, 2021). Conformal prediction is an uncertainty quantification method with coverage guarantees even for misspecified models and a simple mechanism to correct for covariate shift. A conformal

mal prediction set is defined as $C_\alpha(\mathbf{x}) \subset \mathcal{Y}$ is a set of possible labels for a test point \mathbf{x}_n .

Candidate labels y' are included in $C_\alpha(\mathbf{x})$ if the resulting pair (\mathbf{x}_n, y') is sufficiently similar to actual examples seen in the past. The degree of similarity is measured by a score function s and importance weights \mathbf{w} , and the similarity threshold is determined by the miscoverage tolerance α (see (Stanton et al., 2022) for further details).

2.5 Optimized Transformations with Bayesian Optimization

Figure 1 shows the proposed approach. We define three components: the optimization function, the performance metric, and the model parameters. Besides, we used the transformation matrix to set the optimization function (see section 2.2) and the performance metric. Finally, a Gaussian process was selected and tested with different acquisition functions in the Bayesian optimizer block. Our goal is to sample the transformation parameters of the registration process by using the posterior distribution over the acquisition function.

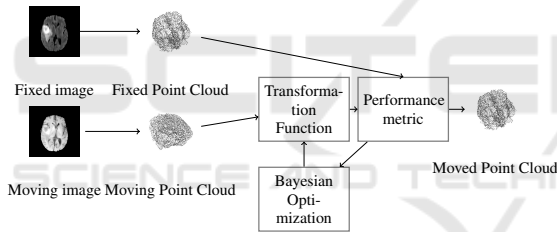


Figure 1: Proposed Approach for optimizing the hyperparameters of an affine transformation function. The model finds the hyperparameters that optimize a performance metric to align the Moving point cloud to the Fixed point cloud.

3 RESULTS AND DISCUSSIONS

Figure 2 shows some point clouds alignment using the Tosca dataset (Bronstein et al., 2006; Bronstein et al., 2007). The results show that Bayesian optimizers can accurately compute affine transformation parameters. For instance, figure 2a and figure 2b show how the model aligns the blue shapes with the red ones. Hence, we can analyze the changes produced from the fixed point cloud to the moving one (i.e., legs and head of the horse).

Besides, the model was also tested with the brain structure dataset as shown in figure 3. Figure 3b and 3d show the resulting shape alignment for two neurodevelopmental cases. We matched both left and right white matter structures at two different times.

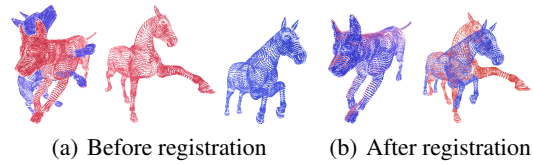


Figure 2: Example of our method with rigid transformations in some point clouds available in Tosca dataset. We analyzed the results of point clouds that present different poses.

As a consequence, significant loss of white matter can be noted when comparing the first and second brain structures (i.e., red and green shapes). Thus, Bayesian optimization computes robust transformation parameters allowing accurate matches and resulting in relevant neurodevelopmental tools for shape quantification.

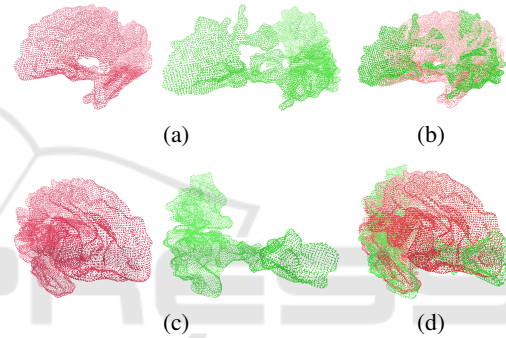


Figure 3: Shape alignment examples for two neurodevelopmental cases. We define the red point clouds as fixed and the green point clouds as the moving ones. The brain structures are left (a-b) and right white matter (c-d).

Figure 4a and figure 4b show the convergence of the Bayesian optimization process for left and right white matter, respectively. The red plots show the distance between the hyperparameters for each iteration. It can be seen in figure 4 the exploration and exploitation behavior during the hyperparameter tuning. Exploration means that the model is sampling the hyperparameters from broad bounded regions. Also, small distances between consecutive hyperparameters indicate the exploitation stage where the fine-tuning is performed. Besides, the blue plots show the minimum error obtained for each iteration. Thus, we analyze how the model initiates a grid search that estimates an optimal solution by performing probabilistic modeling.

Table 1 and 2 show the quantitative results of the alignment process for the two datasets. We report both NMI and RMSE metrics for comparison where the Least-squares estimation (Umeyama, 1991), ICP Employing K-D Tree optimization (Liu et al., 2016), and Point Cloud matching using singular value de-

composition (Oomori et al., 2016) are also tested ¹. In table 1, we evaluate the ability of our model to align point clouds with different poses in the Tosca dataset. Besides, table 2 shows the performance of the methods using the Brain Asphyxia dataset. The results show that ICP-based methods fail on some point clouds making a qualitatively incorrect point cloud alignment as shown in figure 5. The results show that our model outperforms other registration strategies even for large iteration experiments. Consequently, the results show that a Bayesian optimization strategy does not fall into local minima due to its capability of a trade-off between exploitation and exploration, which is controlled by the acquisition function. Hence the compared models lack robustness and exhibit local minima convergences and inaccurate matches.

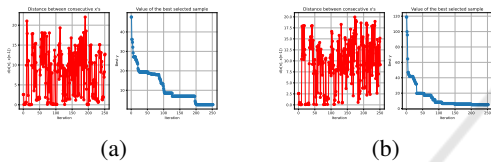


Figure 4: Convergence of the Bayesian Optimization process. The figures show the distance between values of x selected consecutively (red plot), and the minimum value of the performance index obtained in each iteration (blue plot).

Table 1: Comparison with different ICP algorithms. We report Root Mean Square Error (RMSE $\times 10^{-3}$) and Normalized Mutual Information (NMI) using the Tosca dataset

Method	RMSE ↓	NMI ↑
Least-squares Estimation of transformation Parameters Between Two Point Patterns(Umeyama, 1991)	$4.86e^{-7} \pm 4.39e^{-7}$	$0.99 \pm 9.04e^{-5}$
ICP Employing K-D Tree Optimization (Liu et al., 2016)	21.58±32.49	0.76±0.29
Point cloud matching using singular value decomposition (Oomori et al., 2016)	20.60±33.29	0.81±0.28
Our approach	4.20±2.64	0.88±0.08

Table 2: Comparison with different ICP algorithms using the Brain Structure dataset.

Method	RMSE-BS ↓	NMI-BS ↑
Least-squares Estimation of transformation Parameters Between Two Point Patterns(Umeyama, 1991)	76.81±5.21	0.14±0.01
ICP Employing K-D Tree Optimization (Liu et al., 2016)	67.88±8.21	0.21±0.02
Point cloud matching using singular value decomposition (Oomori et al., 2016)	45.29±5.01	$0.24 \pm 4.12e^{-3}$
Our approach	32.29±2.21	0.78±0.05

¹All the mentioned methods were implemented to be tested in the specific datasets of this work, The quantitative results was obtained using all the brain structures of the Brain Asphyxia Dataset

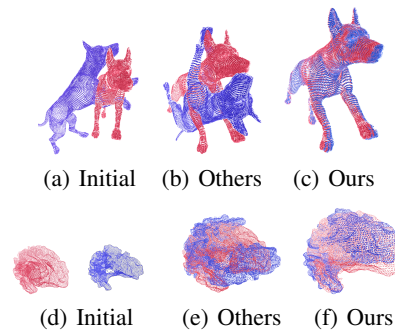


Figure 5: Some alignment processes for both datasets (b) (Liu et al., 2016; Oomori et al., 2016) and (e) (Liu et al., 2016; Oomori et al., 2016; Umeyama, 1991) with the compared approaches. The other methods have problems aligning some point clouds correctly, indicating local optima problems. For instance, figure b and e show moved shapes rotated with respect to the fixed ones (red).

4 CONCLUSIONS

This paper presented a Bayesian Optimization framework for probabilistic 3D shape registration processes. Our method seeks to find the optimal parameters that align point clouds data in a probabilistic way. The experimental results showed that our approach aligns point clouds properly by solving problems usually found in common ICP strategies such as local optima. This approach is relevant for aligning point clouds that are non-rigid, as shown in point clouds of Brain Structures, which allows us to make a more exhaustive analysis of the neurodevelopmental changes that appeared in perinatal asphyxia.

For future works, we plan to analyze to extend this framework on non-rigid shape matching. The motivation for this research line is based on the need to accurately quantify plausible elastic changes related to neurodevelopmental clinical outcomes.

ACKNOWLEDGEMENTS

We thank the Ministry of Sciences of Colombia for financing the project with CTO 897-2021. Also acknowledges to the master’s degree in electrical engineering, vice-rectorate of research, innovation and extension of the technological university of Pereira for its funding with code E6-23-1.

REFERENCES

Balakrishnan, G., Zhao, A., Sabuncu, M., Guttag, J., and Dalca, A. V. (2019). Voxelmorph: A learning

- framework for deformable medical image registration. *IEEE Transactions on Medical Imaging*, 38:1788–1800.
- Besl, P. J. and McKay, N. D. (1992). A method for registration of 3-d shapes. *IEEE Trans. Pattern Anal. Mach. Intell.*, 14:239–256.
- Bouaziz, S., Tagliasacchi, A., and Pauly, M. (2013). Sparse iterative closest point. *Computer Graphics Forum*, 32.
- Bronstein, A. M., Bronstein, M. M., and Kimmel, R. (2006). Efficient computation of isometry-invariant distances between surfaces. *SIAM J. Sci. Comput.*, 28:1812–1836.
- Bronstein, A. M., Bronstein, M. M., and Kimmel, R. (2007). Calculus of nonrigid surfaces for geometry and texture manipulation. *IEEE Transactions on Visualization and Computer Graphics*, 13:902–913.
- Chen, Y. and Medioni, G. (1991). Object modeling by registration of multiple range images. *Proceedings. 1991 IEEE International Conference on Robotics and Automation*, pages 2724–2729 vol.3.
- Dai, Z., Yu, H., Low, K. H., and Jaillot, P. (2019). Bayesian optimization meets bayesian optimal stopping. In *ICML*.
- Fischl, B. R. (2012). Freesurfer. *NeuroImage*, 62:774–781.
- Fong, E. and Holmes, C. C. (2021). Conformal bayesian computation. In *NeurIPS*.
- García, H., Álvarez, M. A., and Orozco, Á. (2016). Bayesian optimization for fitting 3d morphable models of brain structures. In *CIARP*.
- Gutiérrez-Becker, B. and Wachinger, C. (2018). Deep multi-structural shape analysis: Application to neuroanatomy. In *MICCAI*.
- Jaffray, D. A., Kupelian, P. A., Djemil, T., and Macklis, R. (2007). Review of image-guided radiation therapy. *Expert Review of Anticancer Therapy*, 7:103–89.
- Jones, D. R. (2001). A taxonomy of global optimization methods based on response surfaces. *Journal of Global Optimization*, 21:345–383.
- Krebs, J., Delingette, H., Mailhé, B., Ayache, N., and Mansi, T. (2019). Learning a probabilistic model for diffeomorphic registration. *IEEE Transactions on Medical Imaging*, 38:2165–2176.
- Lau, T. F., Luo, J., Zhao, S., Chang, E., and Xu, Y. (2020). Unsupervised 3d end-to-end medical image registration with volume tweening network. *IEEE Journal of Biomedical and Health Informatics*, 24:1394–1404.
- Li, J., Hu, Q., Zhang, Y., and Ai, M. (2022). Robust symmetric iterative closest point. *ISPRS Journal of Photogrammetry and Remote Sensing*, 185:219–231.
- Liu, J., Zhu, J., Yang, J., Meng, X., and Zhang, H. (2016). Three-dimensional point cloud registration based on icp algorithm employing k-d tree optimization. In *International Conference on Digital Image Processing*.
- Mansilla, L., Milone, D. H., and Ferrante, E. (2020). Learning deformable registration of medical images with anatomical constraints. *Neural networks : the official journal of the International Neural Network Society*, 124:269–279.
- Miller, S. P., Ramaswamy, V., Michelson, D. J., Barkovich, A. J., Holshouser, B. A., Wycliffe, N., Glidden, D. V., Deming, D. D., Partridge, J. C., Wu, Y. W., Ashwal, S., and Ferriero, D. M. (2005). Patterns of brain injury in term neonatal encephalopathy. *The Journal of pediatrics*, 146 4:453–60.
- Oliveira, F. P. M. and Tavares, J. (2014). Medical image registration: a review. *Computer Methods in Biomechanics and Biomedical Engineering*, 17:73–93.
- Oomori, S., Nishida, T., and Kurogi, S. (2016). Point cloud matching using singular value decomposition. *Artificial Life and Robotics*, 21:149–154.
- Rasmussen, C. E. and Williams, C. K. I. (2005). *Gaussian Processes for Machine Learning (Adaptive Computation and Machine Learning)*. The MIT Press.
- Rusinkiewicz, M. L. (2001). Efficient variants of the icp algorithm. *Proc. 3rd Int. Conf. 3D Digital Imaging and Modeling*, pages 145–152.
- Sadozye, A. H. and Reed, N. S. (2012). A review of recent developments in image-guided radiation therapy in cervix cancer. *Current Oncology Reports*, 14:519–526.
- Satheesan, A. P., Chinnappa, A. R., Goudar, G., and Raghooji, C. R. (2020). Correlation between early magnetic resonance imaging brain abnormalities in term infants with perinatal asphyxia and neuro developmental outcome at one year. *International Journal of Contemporary Pediatrics*.
- Snoek, J., Larochelle, H., and Adams, R. P. (2012). Practical bayesian optimization of machine learning algorithms. In Pereira, F., Burges, C. J. C., Bottou, L., and Weinberger, K. Q., editors, *Advances in Neural Information Processing Systems 25*, pages 2951–2959. Curran Associates, Inc.
- Stanton, S., Maddox, W. J., and Wilson, A. G. (2022). Bayesian optimization with conformal coverage guarantees. *ArXiv*, abs/2210.12496.
- Umeyama, S. (1991). Least-squares estimation of transformation parameters between two point patterns. *IEEE Trans. Pattern Anal. Mach. Intell.*, 13:376–380.
- Vos, B. D., Berendsen, F., Viergever, M., Sookooti, H., Staring, M., and Isgum, I. (2019). A deep learning framework for unsupervised affine and deformable image registration. *Medical Image Analysis*, 52:12X143.
- Wang, L., Gao, X., Zhou, Z., and Wang, X. (2014). Evaluation of four similarity measures for 2d/3d registration in image-guided intervention. *Journal of Medical Imaging and Health Informatics*, 4:416–421.
- Williams, J. L. and Maybeck, P. (2006). Cost-function-based hypothesis control techniques for multiple hypothesis tracking. *Math. Comput. Model.*, 43:976–989.
- Zhang, J., Yao, Y., and Deng, B. (2022). Fast and robust iterative closest point. *IEEE Transactions on Pattern Analysis and Machine Intelligence*, 44:3450–3466.
- Zhang, P. (2015). Evaluating accuracy of community detection using the relative normalized mutual information. In *Journal of Statistical Mechanics: Theory and Experiment*.
- Zhang, Z. (2005). Iterative point matching for registration of free-form curves and surfaces. *International Journal of Computer Vision*, 13:119–152.
- Zhao, S., Dong, Y., Chang, E., and Xu, Y. (2019). Recursive cascaded networks for unsupervised medical image registration. *2019 IEEE/CVF International Conference on Computer Vision (ICCV)*, pages 10599–10609.